The Little Book of Deep Learning

François Fleuret

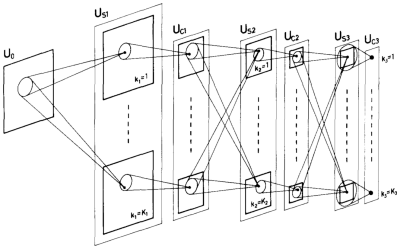

UNIVERSITÉ DE GENÈVE

beta-2023.04.24

François Fleuret is professor of computer science at the University of Geneva, Switzerland.

The cover illustration is the schematic of the Neocognitron by Fukushima [1980], a key ancestor of deep neural networks.

Contents

List of Figures

Foreword

The current period of progress in artificial intelligence was triggered when Krizhevsky et al. [2012] showed that an artificial neural network with a simple structure, that had been known for more than twenty years [LeCun et al., 1989], could beat complex state-of-the-art image recognition methods by a huge margin, simply by being large and trained on a large data set.

This breakthrough was made possible thanks to Graphical Processing Units (GPU), mass-market highly parallel computing devices developed for real-time image synthesis, and repurposed for artificial neural networks.

Since then, under the umbrella term of "deep learning", innovations in the structures of these networks, the strategies to train them and dedicated hardware, have allowed for an exponen-

tial increase in both their size and the quantity of training data they take advantage of [Sevilla et al., 2022]. This resulted in a wave of successful applications across technical domains, from computer vision and robotics, to speech, and natural language processing.

Although the bulk of deep learning is not particularly hard to understand, it combines diverse components, which makes it complicated to learn. It involves multiple branches of mathematics such as calculus, probabilities, optimization, linear algebra, or signal processing, and it also is deeply anchored in computer science, programming, algorithmic, and high-performance computing. Instead of going into details and trying to be exhaustive, this little book is limited to the necessary background and technical tools to understand a few important models.

If you did not get this book from its official url

https://fleuret.org/public/lbdl.pdf

please do so, so that I can estimate the number of readers.

François Fleuret
April 21, 2023

Part I

Foundations

Chapter 1

Machine Learning

Deep learning belongs historically to the larger field of statistical machine learning, as it fundamentally concerns methods able to learn representations from data. However, its modularity, versatility, and scaling qualities, resulted in a plethora of specific mathematical methods and software development tools that established it as a separate and vast technical field.

1.1 Learning from data

The simplest use case for a model trained from data is when a signal x is accessible, for instance the picture of a license plate, from which one wants to predict a quantity y, such as the string of characters written on the plate.

In many real-world situations where x is a high-dimension signal captured in an uncontrolled environment, it is too complicated to come up with an analytical recipe that relates x and y.

What one can do is to collect a large training set $\mathscr{D}$ of pairs (x_n, y_n), and devise a parametric model f, a piece of computer code that incorporates trainable parameters w that modulate its behavior, and such that, with the proper values w^*, it is a good predictor. "Good" here means that if an x is given to this piece of code, the value $\hat{y} = f(x; w^*)$ it computes is a good estimate of the y that would have been associated to x in the training set if they had been there.

This notion of goodness is usually formalized with a loss $\mathscr{L}(w)$ which is small when $f(\cdot; w)$ is good on $\mathscr{D}$. Then, training the model consists of computing a value w^* that minimizes $\mathscr{L}(w^*)$.

The trainable parameters that compose w are

often referred to as weights, by analogy with the synaptic weights of biological neural networks. In addition to these parameters, models usually depend on meta parameters which are set according to domain prior knowledge, best practices, or resource constraints. They may also be optimized in some ways, but with techniques different than those used to optimize w.

1.2 Basis function regression

We can illustrate the training of a model in a simple case where x_n and y_n are two real numbers, the loss is the mean squared error

$$\mathscr{L}(w) = \frac{1}{N}\sum_{n=1}^{N}(y_n - f(x_n;w))^2, \qquad (1.1)$$

and $f(\cdot;w)$ is a linear combination of a predefined basis of functions $f_1,\dots,f_K$, with $w = (w_1,\dots,w_K)$ their respective weights.

Since $f(x_n;w)$ is linear with respect to the w_ks and $\mathscr{L}(w)$ is quadratic with respect to $f(x_n;w)$, the loss $\mathscr{L}(w)$ is quadratic with respect to the w_ks, and finding w^* that minimizes it boils down to solving a linear system. See the Figure 1.1 for an example with Gaussian kernels as f_k.

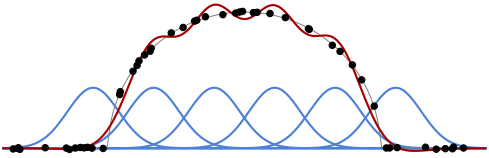

Figure 1.1: *Given a basis of functions (blue curves) and a training set (black dots), we can compute an optimal linear combination of the former (red curve) to approximate the latter for the mean squared error.*

1.3 Categories of models

We can organize the use of machine learning models into three main categories:

• Regression consists of predicting a continuous valued vector $y \in \mathbb{R}^K$, for instance a geometrical position of an object. This is a multi-dimensional generalization of the setup we saw in the previous section. The training set is composed of pairs of an input signal, and a ground truth value.

• Classification aims at predicting a value from a finite set $\{1,\dots,C\}$, for instance an image label. As for regression, the training set is composed of pairs of input signal, and ground truth quantity, here a label from that set. The standard way of tackling this is to predict one score per potential class, such that the correct class has maximum score.

• Density modeling has for objective to model the probability density function of the data μ_X itself, for instance images. In that case the training set is composed of values x_n without associated quantities to predict, and the trained model should allow either to evaluate the probability density function, or to sample from the distribution, or both.

Both regression and classification are generally referred to as supervised learning since the value to predict, which is required as a target during training, has to be produced, for instance by human experts. On the contrary density modeling is usually seen as unsupervised learning since it is sufficient to take existing data, without the need for producing an associated ground-truth.

These three categories are not disjoint, for instance classification can be cast as class score regression, or discrete sequence density modeling as iterated classification. Also, they do not cover all cases. One may want to predict compounded quantities, or multiple classes, or model a density conditional to a signal.

1.4 Under and over-fitting

A key element is the interplay between the capacity of the model, that is its flexibility and ability to fit diverse data, and the amount and quality of the training data. When the capacity is insufficient, the model cannot fit the data and the error during training is high. This is referred to as under-fitting.

On the contrary when the amount of data is insufficient, as shown on Figure 1.2, the performance during training can be excellent, but unrelated to the actual fit to the data structure, as in that case the model will often learn random noise present in the signal. This is over-fitting.

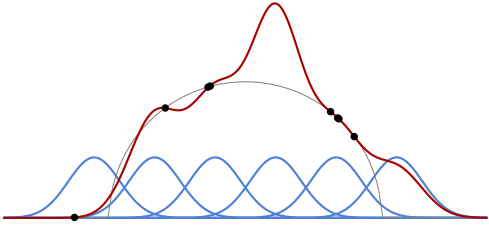

Figure 1.2: *If the amount of training data is small compared to the capacity of the model, the performance during training reflects poorly the actual fit to the underlying data structure, and consequently the usefulness for prediction.*

So a large part of the art of applied machine learning is to design models which are not too flexible, but still able to fit the data. This is done by crafting the right inductive bias in a model, which means that its structure corresponds to the underlying structure of the data at hand.

Even though this classical perspective is relevant for reasonably sized deep models, things get confusing with large ones which have very large number of trainable parameters and extreme capacity, but still perform well for prediction. We will come back to this in § 3.5.

Chapter 2

Efficient computation

From an implementation standpoint, deep learning is about executing heavy computations with large amounts of data, and the Graphical Processing Units (GPU) have been instrumental in the success of the field by allowing such computations to be run on affordable hardware.

The importance of their use, and the resulting technical constraints on the computations that can actually be done efficiently, force the research in the field to constantly balance mathematical soundness and implementability of novel methods.

2.1 GPUs, TPUs, and batches

Graphical Processing Units were originally designed for real-time image synthesis, which requires highly parallel architectures that happen to be fitting to deep models. As their usage for AI has increased, GPUs got equipped with dedicated sub-components referred to as tensor cores, and deep-learning specialized chips such as Google's Tensor Processing Units (TPUs) have been produced.

A GPU possesses several thousands of parallel units, and its own fast memory. The limiting factor is usually not the number of computing units but the read-write operations to memory. The slowest link is between the CPU memory and the GPU memory and consequently one should avoid copying data across devices. Moreover the structure of the GPU itself involves multiple levels of cache memory, which are smaller but faster, and computation should be organized to avoid copies between these different caches.

This is achieved in particular by organizing the computation in batches of samples that are processed in parallel. When an operator combines a sample and model parameters, both have to be moved to the cache memory near the actual computing units. Proceeding by batches allows for

copying the model parameters only once, instead of doing it for every sample. In practice a GPU processes a batch that fits in memory almost as quickly as a single sample.

A standard GPU has a theoretical peak performance of 10^{13}-10^{14} floating point operations (FLOPs) per second, and usually its memory size is between 8 and 80 gigabytes. The standard FP32 encoding of float numbers is on 32 bits but empirical results show that using the FP16 encoding on 16 bits for some operands does not degrade performance.

Typical vision models have 10–100 millions of trainable parameters and require 10^{18}–10^{19} FLOPs for training [He et al., 2015; Sevilla et al., 2022]. Language model have from 100 millions to hundreds of billions of parameters and require 10^{20}–10^{23} FLOPs for training [Devlin et al., 2018; Brown et al., 2020; Chowdhery et al., 2022; Sevilla et al., 2022]. The latter require machines with multiple high-end GPUs.

2.2 Tensors

GPUs and deep learning frameworks such as PyTorch or JAX manipulate the quantities to process by organizing them as tensors, which are series of scalars arranged along several discrete axes. They are elements of $\mathbb{R}^{N_1 \times \cdots \times N_D}$ that generalize the notion of vector and matrix.

Tensors are used to represent both the signals to process, the trainable parameters of the models, and the intermediate quantities they compute. The latters are called activations, in reference to neuronal activations.

A time series for instance is naturally encoded as a $D \times T$ tensor, where T is its duration and D the dimension of the feature representation at every time step, often referred to as the number of channels. Similarly a 2d-structured signal can be represented as a $D \times H \times W$ tensor, where H and W are its width and height. An RGB image would correspond to $D = 3$, but the number of channels can grow up to several thousands in large models.

Adding more dimensions allows for the representation of series of objects. Fifty RGB images of resolution 32×24 can for instance be encoded as a $50 \times 3 \times 24 \times 32$ tensor.

Deep learning libraries all provide a large number of operations that encompass standard linear algebra, complex re-shaping and extraction, and deep-learning specific operations, some of which we will see in Chapter 4. The implementation of tensors separates the shape representation from the storage layout of the coefficients in memory, which allows many re-shaping, transposing, and extraction operations to be done without coefficient copy, hence extremely rapidly. In practice, virtually any computation can be decomposed into elementary tensor operations, which avoids non-parallel loops at the language level, and poor memory management.

Beside being convenient tools, tensors are instrumental in achieving computational efficiency. All the people involved in designing the complex object that is an operational deep model, from the researchers and software developers designing the model, the libraries, and the drivers, to the engineers designing the computers, and the computing chips themselves, everybody knows that the data will be manipulated as tensors. The resulting constraints on locality and block decomposability allow all the actors of this chain to optimize their designs.

Chapter 3

Training

As introduced in § 1.1, training a model consists of minimizing a loss $\mathscr{L}(w)$ which reflects the performance of the predictor $f(\cdot;w)$ on a training set $\mathscr{D}$. Since the models are usually extremely complex, and their performance is directly related to how well the loss is minimized, this minimization is a key challenge both computationally and mathematically.

3.1 Losses

The example of the mean squared error of equation 1.1 is a standard loss for predicting a continuous value.

For classification, the usual strategy is that the output of the model is a vector with one component $f(x;w)_y$ per class y, interpreted as the logarithm of a non-normalized probability, or logit. With X the input signal and Y the class to predict we can then compute from f an estimate of the posterior probabilities:

$$\hat{P}(Y=y \mid X=x) = \frac{\exp f(x;w)_y}{\sum_z \exp f(x;w)_z}. \quad (3.1)$$

This expression is generally referred to as the softmax, or more adequately softargmax, of the logits.

To be consistent with this interpretation the model should be trained to maximize the probability of the true classes, hence to minimize the cross-entropy, expressed as

$$\mathscr{L}_{\text{ce}}(w) = -\frac{1}{N}\sum_{n=1}^{N} \log \frac{\exp f(x_n;w)_{y_n}}{\sum_z \exp f(x_n;w)_z}. \quad (3.2)$$

For density modeling, the standard loss is the likelihood of the data. If $f(x;w)$ is to be inter-

preted as a normalized log-probability or density, the loss is the opposite of the sum of its value over training samples.

In certain setups, even though the value to predict is continuous, the supervision takes the form of ranking constraints. The standard domain is metric learning, where the objective is to learn a measure of distance between samples such that two samples from the same semantic class, e.g. two pictures of a same person, are closer to each other than to a sample from another class, e.g. any picture of someone else. The standard approach for such cases is to minimize a contrastive loss, in that case for instance the sum over triplets (x_a, x_b, x_c), such that $y_a = y_b \neq y_c$, of

$$\max(0, 1 - f(x_a, x_c; w) + f(x_a, x_b; w)). \quad (3.3)$$

This quantity will be strictly positive unless $f(x_a, x_c; w) \geq 1 + f(x_a, x_b; w)$.

It is also possible to add terms to the loss that depend on the trainable parameters of the model themselves to favor certain configurations.

The weight decay regularization for instance consists of adding to the loss a term proportional to the sum of the parameters squared. It can

be interpreted as having a Gaussian Bayesian prior on the parameters which favors smaller parameters, and reduces the influence of the data. This degrades performance on the training set, but reduces the gap between the performance in training and that on new, unseen data.

Usually the loss to minimize is not the actual quantity one want to optimize ultimately, but a proxy for which finding the best model parameters is easier. For instance cross-entropy is the standard loss for classification, even though the actual performance measure is a classification error rate, because the latter has no informative gradient, a key requirement as we will see in § 3.3.

3.2 Autoregressive models

Many spectacular applications in computer vision and natural language processing have been tackled by modeling the distribution of a high-dimension discrete vector with the chain rule:

$$\begin{aligned} &P(X_1 = x_1, X_2 = x_2, \ldots, X_T = x_T) = \\ &\quad P(X_1 = x_1) \\ &\times P(X_2 = x_2 \mid X_1 = x_1) \\ &\quad \ldots \\ &\times P(X_T = x_T \mid X_1 = x_1, \ldots, X_{T-1} = x_{T-1}) \end{aligned} \tag{3.4}$$

When dealing with sequences of discrete tokens from a vocabulary $\{1, \ldots K\}$, and with the convention that the additional token 0 stands for an "unknown" quantity, we can represent the event $\{X_1 = x_1, \ldots, X_t = x_t\}$ as the vector $(x_1, \ldots, x_t, 0, \ldots, 0)$.

Then, given a model

$$\begin{aligned} &f(x_1, \ldots, x_{t-1}, 0, \ldots, 0; w) = \\ &\quad \log \hat{P}(X_t \mid X_1 = x_1, \ldots, X_{t-1} = x_{t-1}), \end{aligned} \tag{3.5}$$

the chain rule states that one can sample a full sequence of length T by sampling the x_ts one after another, each according to the predicted posterior distribution, given the $x_1, \ldots, x_{t-1}$ already

sampled. This is an autoregressive generative model.

Training such a model could be achieved naively by minimizing the sum across training sequences x and time steps t of

$$\mathscr{L}_{\text{ce}}\big(x_t, f(x_1,\dots,x_{t-1},0,\dots,0;w)\big), \qquad (3.6)$$

however such an approach is inefficient, as most computation done for $t < t'$ have to be repeated for t'.

The standard strategy to address this issue is to design a model that predicts the distributions of all the x_t of the sequence at once, but with a structure such that the prediction of x_t's logits depends only on the input values $x_1,\dots,x_{t-1}$. Such a model is called causal, since it corresponds in the case of temporal series to not letting the future influence the past. As we will see in § 7.1, it can be trained with the cross-entropy summed over all the time steps for every sequence processed.

3.3 Gradient descent

Except in specific cases like the linear regression we saw in the previous chapter, the optimal parameters w^* do not have a closed form expression. In the general case the tool of choice to minimize a function is gradient descent. It consists of initializing the parameters with a random w_0, and then improving this estimate by iterating gradient steps, each consisting of computing the gradient of the loss with respect to the parameters, and subtracting a fraction of it

$$w_{n+1} = w_n - \eta \nabla \mathscr{L}_{|w}(w_n). \tag{3.7}$$

This procedure corresponds to moving the current estimate a bit in the direction corresponding locally to the maximum decrease of $\mathscr{L}(w)$, as illustrated on Figure 3.1.

The meta parameter η is referred to as the learning rate. It is a positive value that modulates how quickly the minimization is done, and has to be chosen carefully. If it is too small, the optimization will be slow at best, and may be trapped in a local minimum early. If it is too large the optimization may bounce around a good minimum and never descend into it. As we will see in § 3.5, it can depend on the iteration number n.

All the losses used in practice can be expressed

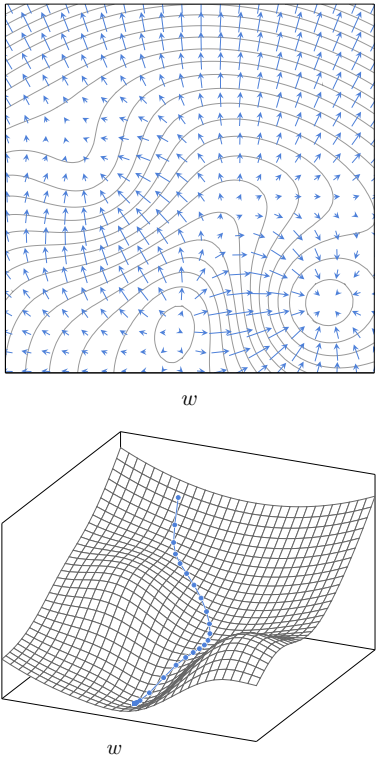

Figure 3.1: *At every point w, the gradient $\nabla\mathscr{L}_{|w}(w)$ is in the direction that maximizes the increase of $\mathscr{L}$, orthogonal to the level curves (top). The gradient descent minimizes $\mathscr{L}(w)$ iteratively by subtracting a fraction of the gradient at every step, resulting in a trajectory that follows the steepest descent (bottom).*

as an average of a per-sample loss

$$\mathscr{L}(w) = \frac{1}{N}\sum_{n=1}^{N} \ell_n(w), \tag{3.8}$$

where $\ell_n(w) = L(f(x_n; w), y_n)$ for some L, and the gradient is then

$$\nabla\mathscr{L}_{|w}(w) = \frac{1}{N}\sum_{n=1}^{N} \nabla\ell_{n|w}(w). \tag{3.9}$$

The resulting gradient descent would compute exactly the sum in 3.9, which is usually computationally heavy, and then update the parameters according to 3.7. However, under reasonable assumptions of exchangeability, for instance if the samples have been properly shuffled, any partial sum of 3.9 is an unbiased estimator of the full sum, albeit noisy. So updating the parameters from partial sums corresponds to doing more gradient steps for the same computational budget, with noisier estimates of the gradient. Due to the redundancy in the data, this happens to be a far more efficient strategy. We saw in § 2.1 that processing a batch of samples is generally as fast as processing a single one. Hence the standard approach is to split the full set $\mathscr{D}$ into batches, and to update the parameters from the estimate

of the gradient computed from each. This is referred to as mini-batch stochastic gradient descent, or stochastic gradient descent (SGD) for short.

It is important to note that this process is extremely gradual and that the number of mini-batches and gradient steps are typically of the order of several millions.

Plenty of variations of this standard strategy have been proposed. The most popular one is Adam [Kingma and Ba, 2014], which keeps running estimates of the mean and variance of each component of the gradient, and normalizes them automatically, avoiding scaling issues and different training speeds in different parts of a model.

3.4 Backpropagation

Using gradient descent requires a technical means to compute $\nabla \ell_{n|w}(w)$. Given that f and L are both compositions of standard tensor operations, as for any mathematical expression, the chain rule allows us to get an expression of it.

Consider the simple case of a composition of mappings

$$f = f_1 \circ f_2 \circ \cdots \circ f_D.$$

The output of f can be computed by applying the f_ds one after another, and computing the out-

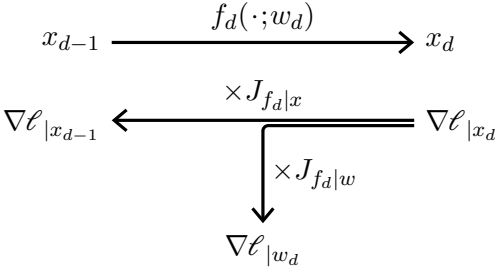

Figure 3.2: *Given a model $f = f_D \circ \cdots \circ f_1$, the forward pass (top) consists of computing the outputs x_d of the mappings f_d in order. The backward pass (bottom) computes the gradients of the loss with respect to the activation x_d and the parameters w_d backward by multiplying them by the Jacobians.*

put x_d of each. In reference to neural networks, the individual scalar values of these intermediate results are traditionally called activations in reference to neuron activations, the individual mappings are referred to as layers, as we will see is § 4.1, and their sequential evaluation is the forward pass, see Figure 3.2, top.

Conversely the gradient $\nabla \ell_{|x_{d-1}}$ of the loss with respect to the output x_{d-1} of f_{d-1} is the product of the gradient $\nabla \ell_{|x_d}$ with respect to the output of f_d multiplied by the Jacobian $J_{f_{d-1}|x}$ of f_{d-1} with respect to x. So the gradients with respect to the outputs of all the f_ds can be computed recursively backward. And the gradient $\nabla \ell_{|w_d}$ with respect to w_d is the gradient with respect to the output of f_d multiplied by the Jacobian $J_{f_d|w}$ of f_d with respect to w_d. This is the backward pass, see Figure 3.2, bottom.

The combination of this computation of the gradient and gradient descent is often refer to as backpropagation.

In practice the implementation details of the forward and backward passes are hidden from programmers. Deep learning frameworks are able to automatically construct the sequence of operations to compute gradients. A particularly

convenient algorithm is autograd [Baydin et al., 2015], which tracks tensor operations, and builds on the fly the combination of operators for gradients. Thanks to this, a piece of imperative programming that manipulates tensors can automatically compute the gradient of any quantity with respect to any other.

Regarding the computational cost, as we will see, the bulk of the computation goes into linear operations that require one matrix product for the forward pass, and two for the products by the Jacobians for the backward pass. This makes the latter roughly twice more costly than the former.

The memory requirement during inference is equal roughly to that of the most demanding individual layer. For training however, the backward pass requires to keep the activations computed during the forward to compute the Jacobians, which results in a memory usage that grows proportionally to the model's depth. Techniques exist to trade the memory usage for computation by storing the activations for some layers only, and recomputing the others on the fly during the backward pass [Chen et al., 2016].

A key historical issue when training a large net-

work is that when the gradient propagates backwards through many operators it may decrease or increase exponentially. When it decreases exponentially this is called the vanishing gradient, and it may make the training impossible, or in its milder form, make different parts of the model being updated at different speeds, degrading their co-adaptation [Glorot and Bengio, 2010]. As we will see, several techniques have been developed to prevent this from happening.

3.5 Training protocols

Training a deep network requires defining a protocol to make the most of computation and data, and ensure that performance will be good on new data.

As we saw in § 1.4, the performance on the training samples may be misleading, so in the simplest setup one needs at least two sets of samples: one is a training set used to optimize the model parameters, and the other is a test set to estimate the performance of the trained model.

Additionally, there are usually meta parameters to adapt, in particular related to the model architecture, the learning rate, and the regularization terms in the loss. In that case one needs a validation set disjoint from both the training set and the test set to assess what the best setup is.

The full training is usually decomposed in epochs, each of them corresponding to going through all the training examples once. The usual dynamic of the losses is that the train loss decreases as long as the optimization runs while the validation loss may reach a minimum after a certain number of epochs and then starts to increase, reflecting an over-fitting regime, as introduced in § 1.4 and illustrated on Figure 3.3.

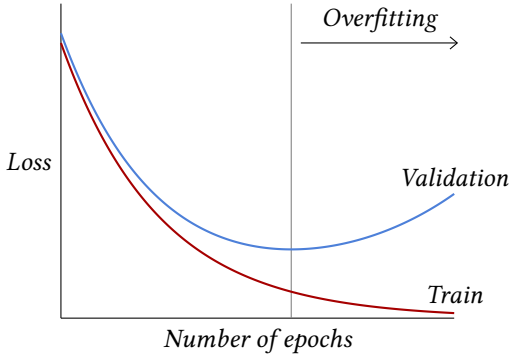

Figure 3.3: *As training progresses, a model's performance is usually monitored through losses. The train loss is the one driving the optimization process and goes down, while the validation loss is estimated on an other set of examples to assess the over-fitting of the model. This phenomenon appears when the model starts to take into account random structures specific to the training set at hands, resulting in the validation loss starting to increase.*

Paradoxically, although they should suffer from severe over-fitting due to their capacity, large models usually continue to improve as the training progresses. This may be due to the inductive bias of the model becoming the main driver of the optimization when the performance is near perfect on the training set [Belkin et al., 2018].

An important design choice is the learning rate

schedule during training. The general policy is that the learning rate should be initially large to avoid having the optimization being trapped in a bad local minimum early, and that it should get small so that the optimized parameter values do not bounce around, and reaches a good minimum in a narrow valley of the loss landscape.

3.6 Training data

One key aspect of deep learning is the steady improvement of performance with the training set size, even in the multi-billions of samples regime.

This is in part due to the structural plasticity of models, that allows to scale them up, as we will see, by increasing the number of layers or feature dimensions. But it is also made possible by the distributed nature of these models, that can take advantage of massively parallel computing devices, and by the stochastic gradient descent, which accesses only a tiny fraction of the data at a time, and can operate with data sets whose size is orders of magnitude greater than that of

Dataset	Year	Nb. of images	Size
ImageNet	2012	1.2M	150Gb
Cityscape	2016	25K	60Gb
LAION-5B	2022	5.8B	240Tb
Dataset	**Year**	**Nb. of books**	**Size**
WMT-18-de-en	2018	14M	8Gb
The Pile	2020	1.6B	825Gb
OSCAR	2020	12B	6Tb

Table 3.1: *Some examples of publicly available datasets. The equivalent number of books is an indicative estimate for 250 pages of 2000 characters per book.*

the computing device's memory.

This has resulted in a tension between producing datasets of moderate size with a detailed and expensive to produce ground-truth, and datasets which are automatically produced by combining automatically data available on the internet with minimal curation, if any. The later category includes datasets that combine multiple modalities, for instance text and images from web pages, or sound and images from videos, which can be used for large scale supervised training.

The current most impressive successes of artificial intelligence with deep learning methods rely on extremely large text datasets, see Table 3.1.

Part II

Deep models

Chapter 4

Model components

A deep model is nothing more than a complicated tensorial computation that can be decomposed ultimately into standard mathematical operations from linear algebra and analysis.

Through the years, the field has developed a large collection of high-level modules that have a clear semantic, and complex models combining these modules, which have proven to be efficient in specific application domains.

4.1 The notion of layer

We call layers standard complex compounded tensor operations that have been designed and empirically identified as being generic and efficient. They often incorporate trainable parameters, and correspond to a convenient level of granularity to design and describe large deep models. The term is inherited from the simple multi-layer neural networks, even though a modern model may take the form of a complex graph of such modules, and incorporates multiple parallel pathways.

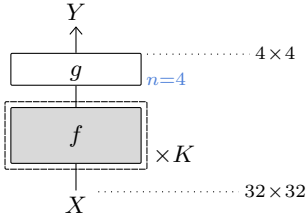

In the following pages I try to stick to the convention for model depiction illustrated above that:

- operators / layers are depicted as boxes,

- darker coloring indicates that they embed trainable parameters,

- non-default valued meta-parameters are added in blue on their right,

- a dashed box with a multiplicative factor indicates that a group of layers is replicated in series, each with its own set of trainable parameters if any, and

- the dimension of their output is specified on the right when it differs from their input.

Additionally, layers that have a complex internal structure are depicted with a greater height.

4.2 Linear layers

Linear layers are the most important modules in terms of computation and number of parameters. They benefit from decades of research and engineering in algorithmic and chip design for matrix operations.

Fully connected layers

The most basic one is the fully connected layer, parameterized by $w = (W, b)$, where W is a $D' \times D$ weight matrix, and b is a bias vector of dimension D'. It implements a matrix/vector products generalized to arbitrary tensor shape. Given an input X of dimension $D_1 \times \cdots \times D_K \times D$, it computes an output Y of dimension $D_1 \times \cdots \times D_K \times D'$ with

$$\forall d_1, \ldots, d_K, \quad Y[d_1, \ldots, d_K] = WX[d_1, \ldots, d_K] + b. \quad (4.1)$$

While at first sight such an affine operation seems limited to geometric transformations such as rotations or symmetries, they can implement far more than that. In particular projections for dimension reduction, or signal filtering, but also from the perspective of the dot product being a measure of similarity, a matrix-vector product can be interpreted as computing matching scores

between a query as encoded by the vector, and keys as encoded by the matrix rows.

As we saw in § 3.3, the gradient descent starts with the parameters' random initialization. If this is done too naively, as seen in § 3.4, the network may suffer from exploding or vanishing activations and gradients [Glorot and Bengio, 2010]. Deep learning frameworks implement initialization methods that modulate the random parameters' scales according to the tensor shape to prevent pathological behaviors of the signal during the forward and the backward passes.

Convolutional layers

A linear layer can take as input an arbitrarily shaped tensor by reshaping it into a vector, as long as it has the right number of coefficients. However such a layer is poorly adapted to dealing with large tensors since the number of parameters and number of operations are proportional to the product of the input and output dimensions. For instance to process an RGB image of size 256×256 as input and compute a result of same size, it would require $\simeq 4 \times 10^{10}$ parameters and multiplications.

Beside these practical issues most of the high-dimension signals are strongly structured. For

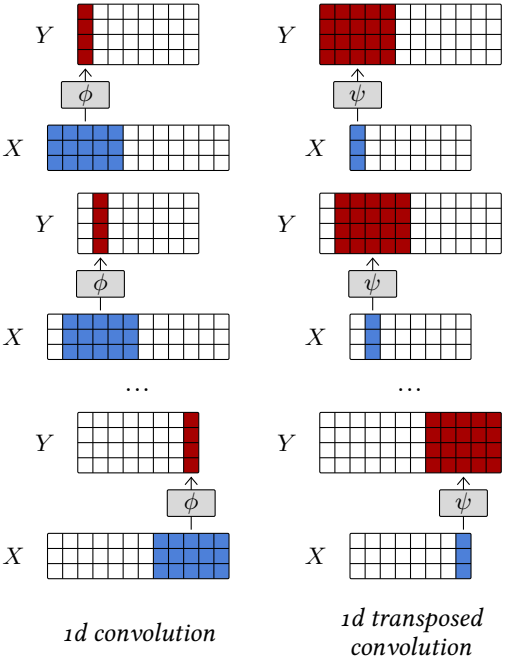

Figure 4.1: *A 1d convolution (left) takes as input a $D \times T$ tensor X, applies the same affine mapping $\phi(\cdot; w)$ to every sub-tensor of shape $D \times K$, and stores the resulting $D' \times 1$ tensors into Y. A 1d transposed convolution (right) takes as input a $D \times T$ tensor, applies the same affine mapping $\psi(\cdot; w)$ to every sub-tensor of shape $D \times 1$, and sums the shifted resulting $D' \times K$ tensors. Both can process inputs of different size.*

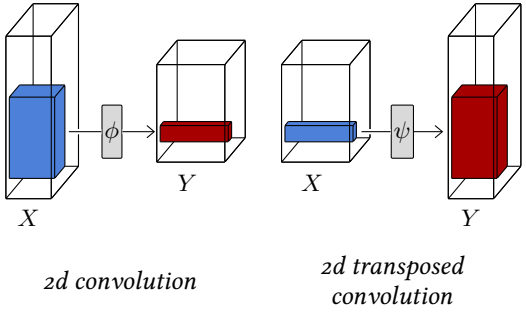

Figure 4.2: *A 2d convolution (left) takes as input a $D \times H \times W$ tensor X, applies the same affine mapping $\phi(\cdot; w)$ to every sub-tensor of shape $D \times K \times L$, and stores the resulting $D' \times 1 \times 1$ tensors into Y. A 2d transposed convolution (right) takes as input a $D \times H \times W$ tensor, applies the same affine mapping $\psi(\cdot; w)$ to every $D \times 1 \times 1$ sub-tensor, and sums the shifted resulting $D' \times K \times L$ tensors into Y.*

instance images exhibit short-term correlations, and statistical stationarity to translation, scaling, and certain symmetries. This is not reflected in the inductive bias of a fully connected layer, which totally ignores the signal structure.

To leverage these regularities, the tool of choice are convolutional layers, which are also affine, but process time-series or 2d signals locally, with the same operator everywhere.

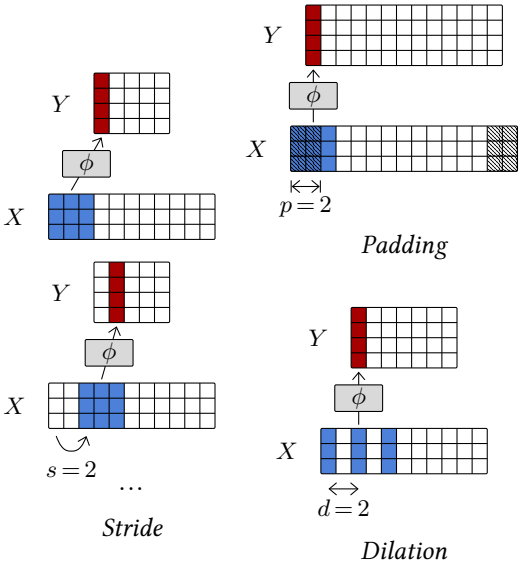

Figure 4.3: *Beside its kernel size and number of input / output channels, a convolution admits three meta-parameter: the stride s (left) modulates the step size when going though the input tensor, the padding p (top right) specifies how many zeros entries are added around the input tensor before processing it, and the dilation d (bottom right) parameterizes the index count between coefficients of the filter.*

A 1d convolution is mainly defined by three meta-parameters: its kernel size K, its number of input channels D, its number of output channels D', and by the trainable parameters w of an affine mapping $\phi(\cdot;w) : \mathbb{R}^{D\times K} \to \mathbb{R}^{D'\times 1}$.

It can process any tensor X of size $D \times T$ with $T \geq K$, and applies $\phi(\cdot;w)$ to every sub-tensor $D \times K$ of X and stores the results into a tensor Y of size $D' \times (T-K+1)$, as pictured on Figure 4.1 (left).

A 2d convolution is similar but has a $K \times L$ kernel and takes as input a $D \times H \times W$ tensor, see Figure 4.2 (left).

Both operators have for trainable parameters those of ϕ that can be envisioned as D' filters of size $D \times K$ or $D \times K \times L$ respectively, and a bias vector of dimension D'.

They also admit three additional meta-parameters, illustrated on Figure 4.3:

- The padding specifies how many zeros coefficients should be added around the input tensor before processing it, in particular to maintain the tensor size when the kernel size is greater than one. Its default value is 0.

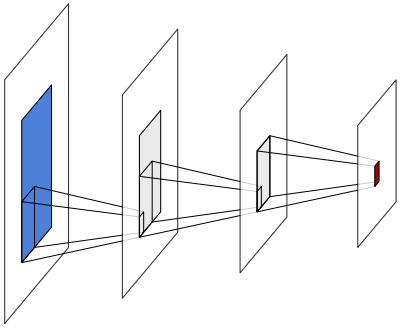

Figure 4.4: *Given an activation in a series of convolution layers, here in red, its receptive field is the area in the input signal, in blue, that modulates its value. Each intermediate convolutional layer increases its size by roughly half its kernel size.*

- The stride specifies the step used when going through the input, allowing to reduce the output size geometrically by using large steps. Its default value is 1.

- The dilation specifies the index count between the filter coefficients of the local affine operator. Its default value is 1, and greater values correspond to inserting zeros between the coefficients, which increases the filter / kernel size while keeping the number of trainable parameters unchanged.

Except for the number of channels, a convolu-

tion's output is usually strictly smaller than its input by roughly the size of the kernel, or even by a scaling factor if the stride is greater than one. Convolutions are used to recombine information, generally to reduce the spatial size of the representation, trading it for a greater number of channels, that translates into a richer local representation. They can implement differential operators such as edge-detectors, or template matching mechanisms. A succession of such layers can also be envisioned as a compositional and hierarchical representation [Zeiler and Fergus, 2014], or as a diffusion process in which information can be transported by half the kernel size when going through a layer.

Given an activation computed by a convolutional layer, or the vector of values for all the channels at a certain location, the portion of the input signal that it depends on is called its receptive field. See Figure 4.4. One of the $H \times W$ subtensors corresponding to a single channel of a $D \times H \times W$ activation tensor is referred to as an activation map.

A converse operation is the transposed convolution that consists also in a localized affine operator, defined by similar meta and trainable parameters as the convolution, but which ap-

plies, for instance in the 1d case, an affine mapping $\psi(\cdot; w) : \mathbb{R}^{D \times 1} \to \mathbb{R}^{D' \times K}$, to every $D \times 1$ sub-tensor of the input, and sums the shifted $D' \times K$ resulting tensors to compute its output. Such operator increases the size of the signal and can be understood intuitively as a synthesis process. See Figure 4.1 (right) and 4.2 (right).

A series of convolutional layers is the usual architecture to map a large dimension signal such as an image or a sound sample to a low dimension tensor. That can be for instance to get class scores for classification, or a compressed representation. Transposed convolutions layers are used the opposite way to build a large dimension signal from a compressed representation, either to assess that the compressed representation contains enough information to build back the signal, or for synthesis, as it is easier to learn a density model over a low dimension representation. We will come back to this in 5.2.

4.3 Activation functions

If a network was combining only linear components it would itself be a linear operator, so it is essential to have non-linear operations. They are implemented in particular with activation functions which are layers that transforms every component of the input tensor individually through a mapping, resulting in a tensor of same shape.

There are many different activation functions but the most used is the Rectified Linear Unit (ReLU, [Glorot et al., 2011]), which sets negative values to zero and keeps positive values unchanged, see Figure 4.5 (top right):

$$\text{relu}(x) = \begin{cases} 0 & \text{if } x < 0 \\ x & \text{otherwise.} \end{cases} \tag{4.2}$$

Given that the core training strategy of deep-learning relies on the gradient, it may seem problematic to have a mapping that is not differentiable at zero, and constant on half the real line. However, the main property gradient descent requires is that the gradient is informative on average. Parameter initialization and data normalization make half of the activations positive when the training starts, ensuring that this is the case.

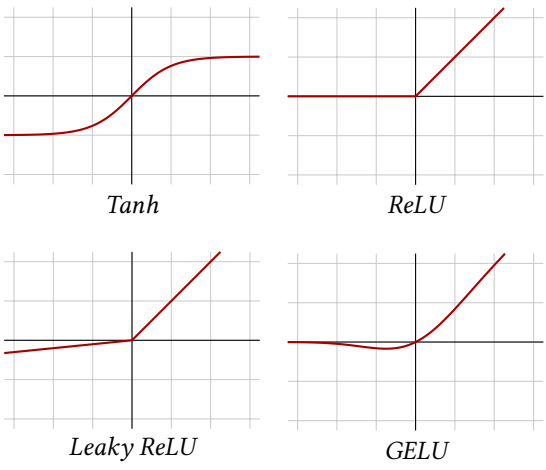

Figure 4.5: *Activation functions.*

Before the generalization of ReLU, the standard activation function was Tanh, see Figure 4.5 (top left) which saturates exponentially fast on both the negative and the positive side, which was aggravating the vanishing gradient.

Other popular activation functions follow the same idea of keeping positive values unchanged and squashing the negative values. Leaky ReLU [Maas et al., 2013] applies a small positive multiplying factor to the negative values, see Figure

4.5 (bottom left).

$$\text{leakyrelu}(x) = \begin{cases} ax \text{ if } x < 0 \\ x \text{ otherwise.} \end{cases} \tag{4.3}$$

And GELU [Hendrycks and Gimpel, 2016] is defined with the cumulative distribution function of the Gaussian distribution, and roughly behaves like a smooth ReLU, see Figure 4.5 (bottom right).

$$\text{gelu}(x) = xP(Z \leq x), \tag{4.4}$$

where $Z \sim \mathcal{N}(0,1)$.

The choice of an activation function, in particular among the variants of ReLU, is generally driven by empirical performance.

4.4 Pooling

A classical strategy to reduce the signal size is to use a pooling operation that combines multiple activations into one that ideally summarizes the information. The most standard operation of this class is the max pooling layer which, similarly to convolution, can operate in 1d and 2d, and is defined by a kernel size.

This layer computes the maximum activation per channel, over non-overlapping sub-tensors of spatial size equal to the kernel size. These values are stored into a result tensor with the same number of channels as the input, and whose spatial size is divided by the kernel size. As the convolution, this operator has three meta-parameters padding, stride, and dilation, with the stride being equal to the kernel size by default.

The max operation can be intuitively interpreted as a logical disjunction, or when it follows a series of convolutional layer that compute local scores for the presence of parts, as a way of encoding that at least one instance of a part is present. It loses precise location, which makes it invariant to local deformations.

A standard alternative is the average pooling layer that computes the average instead of the

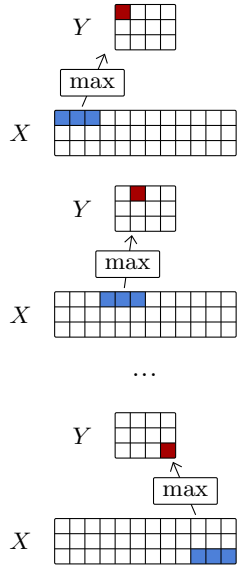

1d max pooling

Figure 4.6: *A 1d max pooling takes as input a $D \times T$ tensor X, computes the max over non-overlapping $1 \times L$ sub-tensors and stores the values in a resulting $D \times (T/L)$ tensor Y.*

max over the sub-tensors. This is a linear operation, while max pooling is not.

4.5 Dropout

Some layers have been designed to explicitly facilitate training, or improve the quality of the learned representations.

One of the main contributions of that sort was dropout [Srivastava et al., 2014]. Such a layer has no trainable parameter but one meta-parameter p, and takes as input a tensor of arbitrary shape.

It is usually switched off during test, in which case its output is equal to its input. When it is active, it has a probability p to set to zero each activation of the input tensor independently, and it re-scales all the activations by a factor $\frac{1}{1-p}$ to maintain the expected value unchanged. See Figure 4.7.

The motivation behind dropout is to favor meaningful individual activation and discourage group representation. Since the probability that a group of k activations remains intact through a dropout layer is $(1-p)^k$, joint representations get unreliable, which makes the training procedure avoid them. It can also be seen as a noise injection that makes the training more robust.

When dealing with images and 2d tensors, the short-term correlation of the signals and the re-

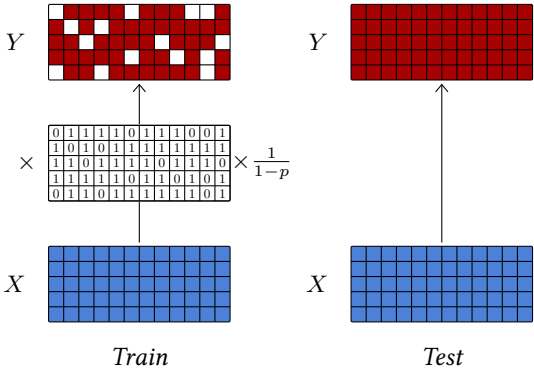

Figure 4.7: *Dropout can process a tensor of arbitrary shape. During training (left), it sets activations at random to zero with probability p and applies a multiplying factor to keep the expected values unchanged. During test (right), it keeps all the activations unchanged.*

sulting redundancy negates the effect of dropout since activations set to zero can be inferred from their neighbors. Hence, dropout for 2d tensors sets entire channels to zero instead of individual activations.

Although dropout is generally used to improve training and is inactive during inference, it can be used in certain setups as a randomization strategy, for instance to estimate empirically confidence scores [Gal and Ghahramani, 2015].

4.6 Normalizing layers

An important class of operators to facilitate the training of deep architectures are the normalizing layers which force the empirical mean and variance of groups of activations.

The main layer in that family is batch normalization [Ioffe and Szegedy, 2015] which is the only standard layer to process batches instead of individual samples. It is parameterized by a meta-parameter D and two series of trainable scalar parameters $\beta_1,\ldots,\beta_D$ and $\gamma_1,\ldots,\gamma_D$.

Given a batch of B samples $x_1,\ldots,x_B$ of dimension D, it first computes for each of the D components an empirical mean $\hat{m}_d$ and variance $\hat{v}_d$ across the batch

$$\hat{m}_d = \frac{1}{B}\sum_{b=1}^{B} x_{b,d} \tag{4.5}$$

$$\hat{v}_d = \frac{1}{B}\sum_{b=1}^{B} (x_{b,d}-\hat{m}_d)^2 \tag{4.6}$$

from which it computes for every component $x_{b,d}$ a normalized value $z_{b,d}$, with empirical mean 0 and variance 1, and from it the final result value $y_{b,d}$ with mean β_d and standard de-

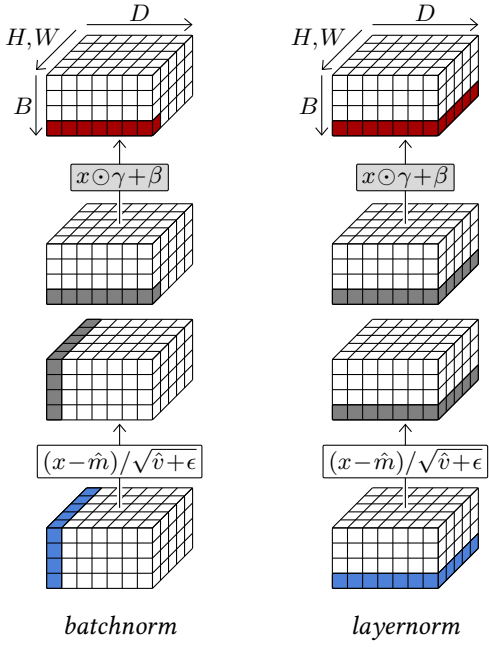

Figure 4.8: *Batch normalization normalizes across the sample index dimension B and all spatial dimensions if any, so B, H, W for a $B \times D \times H \times W$ batch tensor, and scales/shifts according to D, which is implemented as a component-wise product by γ and a sum with β of the corresponding sub-tensors (left). Layer normalization normalizes across D and spatial dimensions, and scales/shifts according to the same (right).*

viation γ_d

$$z_{b,d} = \frac{x_{b,d} - \hat{m}_d}{\sqrt{\hat{v}_d + \epsilon}} \tag{4.7}$$

$$y_{b,d} = \gamma_d z_{b,d} + \beta_d. \tag{4.8}$$

Because this normalization is defined across a batch, it is done only during training. During test, the layer transforms individual samples according to the $\hat{m}_d$s and $\hat{v}_d$s estimated with a moving average over the full training set, which boils down to a fix affine transformation per-component.

The motivation behind batch normalization was to avoid that a change of scaling in an early layer of the network during training impacts all the layers that follow, that then have to adapt their trainable parameters accordingly. Although the real mode of action may be more complicated than this initial motivation, this layer facilitates considerably the training of deep models.

In the case of 2d tensors, to follow the principle of convolutional layers of processing all locations similarly, the normalization is done per-channel across all 2d positions, and β and γ remain vectors of dimension D so that the scaling/shift does not depend on the 2d position. Hence if the tensor to process is of shape

$B \times D \times H \times W$, the layer computes $(\hat{m}_d, \hat{v}_d)$, for $d = 1, \ldots, D$ from the corresponding $B \times H \times W$ slice, normalizes it accordingly, and finally scales and shifts its components with the trainable parameters β_d and γ_d.

So, given a $B \times D$ tensor, batch normalization normalizes it across B and scales/shifts it according to D, which can be implemented as a component-wise product by γ and a sum with β. Given a $B \times D \times H \times W$ it normalizes across B, H, W and scales/shifts according to D, see Figure 4.8, left.

This can be generalized depending on these dimensions. For instance layer normalization [Ba et al., 2016], computes moments and normalizes across all components of individual samples, and scale and shift components individually, see Figure 4.8, right. So, given a $B \times D$ tensor, it normalizes across D, and scales/shifts also according to D. Given a $B \times D \times H \times W$ tensor, it normalizes it across D, H, W and scales/shifts according to the same.

Contrary to batch normalization, since it processes samples individually, it behaves the same during training and test.

4.7 Skip connections

Another technique that mitigates the vanishing gradient and allows the training of deep architecture are the skip connections [Long et al., 2014; Ronneberger et al., 2015]. They are not layers per se, but an architectural design in which outputs of some layers are transported as-is to other layers further in the model, bypassing processing in-between. This unmodified signal can be concatenated or added to the input to the layer the connection branches into. See Figure 4.9. A particular type of skip connections are the residual connections which combine the signal with a sum, and usually skip only a few layers. See Figure 4.9, right.

The main desirable property of this design is to ensure that, even in the case of gradient-killing processing at a certain stage, the gradient will still propagate through the skip connections. Residual connections in particular allow to build deep models with up to several hundreds layers, and key models, such as the residual networks [He et al., 2015] in computer vision, see § 5.2, and the Transformers [Vaswani et al., 2017] in natural language processing, see § 5.3, are entirely composed of blocks of layers with residual connections.

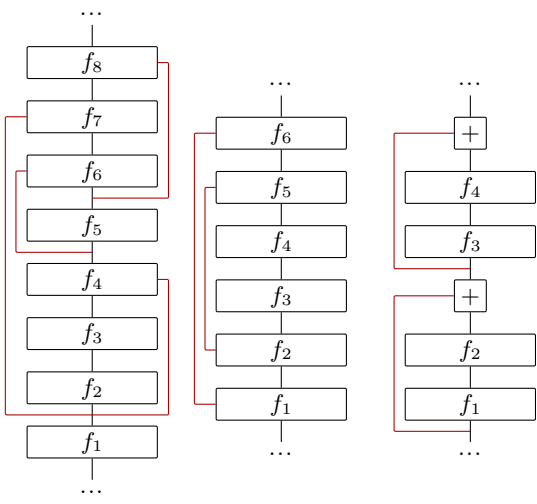

Figure 4.9: *Skip connections, highlighted in red on this figure, transport the signal unchanged across multiple layers. Some architectures (center) that downscale and re-upscale the representation size to operate at multiple scales, have skip connections to feed outputs from the early parts of the network to later layers operating at the same scales [Long et al., 2014; Ronneberger et al., 2015]. The residual connections (right) are a special type of skip connections that sum the original signal to the transformed one, and are usually short-term, bypassing at max a handful of layers [He et al., 2015].*

Their role can also be to facilitate multi-scale reasoning in models that reduce the signal size before re-expanding it, by connecting layers with compatible size. In the case of residual connections, they may also facilitate the learning by simplifying the task to finding a differential improvement instead of a full update.

4.8 Attention layers

In many applications there is a need for a processing able to combine local information at locations far apart in a tensor. This can be for instance distant details for coherent and realistic image synthesis, or words at different positions in a paragraph to make a grammatical or semantic decision in natural language processing.

Fully connected layers cannot process large dimension signals, nor signals of variable size, and convolutional layers are not able to propagate information quickly. Strategies that aggregate the results of convolutions, for instance by averaging them over large spatial areas, suffer from mixing multiple signals into a limited number of dimensions.

Attention layers are specifically addressing this problem by computing for every component of the resulting tensor an attention score to every component of the input tensor, without locality constraints, and averaging features across the full tensor accordingly [Vaswani et al., 2017].

Even though they are substantially more complicated than other layers, they have become a standard element in many recent models. They are in particular the key building block of Trans-

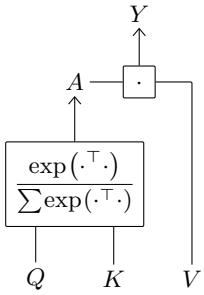

Figure 4.10: *The attention operator* $Y = \mathrm{att}(Q,K,V)$ *computes first an attention matrix* A *as the per-query* $\mathrm{softargmax}$ *of* $Q^\top K$*, and then computes the product between* A *and* V*. See equation 4.11. This operator can be made causal by forcing all the upper-diagonal terms of the matrix* A *to zero before the normalization.*

formers, the dominant architecture for large language models. See § 5.3 and § 7.1.

Attention operator

Given

- a tensor Q of queries of size $N^{\mathtt{Q}} \times D^{\mathtt{QK}}$,
- a tensor K of keys of size $N^{\mathtt{KV}} \times D^{\mathtt{QK}}$, and
- a tensor V of values of size $N^{\mathtt{KV}} \times D^{\mathtt{V}}$,

the attention operator computes a tensor

$$Y = \mathrm{att}(K,Q,V)$$

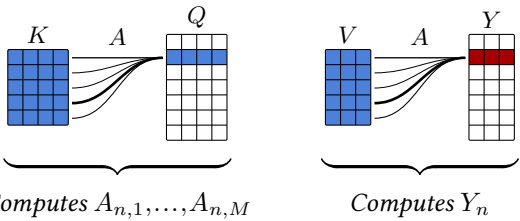

Figure 4.11: *The attention operator can be interpreted as matching every query Q_n with all the keys $K_1,\ldots,K_M$ to get normalized attention scores $A_{n,1},\ldots,A_{n,M}$ (left, and equation 4.9), and then averaging the values $V_1,\ldots,V_M$ with these scores to compute the resulting Y_n (right, and equation 4.10).*

of dimension $N^{\mathrm{Q}} \times D^{\mathrm{V}}$. To do so, it first computes for every query index n and every key index m an attention score $A_{n,m}$ as the softargmax of the dot products between the query Q_n and the keys:

$$A_{n,m} = \frac{\exp\left(\frac{1}{\sqrt{D^{\mathrm{QK}}}} Q_n^\top K_m\right)}{\sum_r \exp\left(\frac{1}{\sqrt{D^{\mathrm{QK}}}} Q_n^\top K_r\right)}, \tag{4.9}$$

where the scaling factor $\frac{1}{\sqrt{D^{\mathrm{QK}}}}$ keeps the range of values roughly unchanged even for large D^{QK}.

Then a retrieved value is computed for each query by averaging the values according to the

attention scores

$$Y_n = \sum_m A_{n,m} V_m. \tag{4.10}$$

See Figure 4.10. So if a query Q_n matches one key K_m far more than all the others, the corresponding attention score $A_{n,m}$ will be close to one, and the retrieved value Y_n will be the value V_m associated to that key. But if it matches several keys equally, then Y_n will be the average of the associated values.

This computation can be implemented efficiently as

$$\mathrm{att}(Q,K,V) = \underbrace{\mathrm{softargmax}\left(\frac{QK^\top}{\sqrt{D^{QK}}}\right)}_{A} V. \tag{4.11}$$

This operator can be made causal by forcing the attention matrix to be lower-diagonal, allowing Y_n to depend only and keys and values of indices less then or equal to n.

Multi-head Attention Layer

This parameter-less attention operator is the key element in the multi-head attention layer depicted in Figure 4.12. This layer has for meta-parameters a number H of heads, and the shapes of three series of H trainable weight matrices

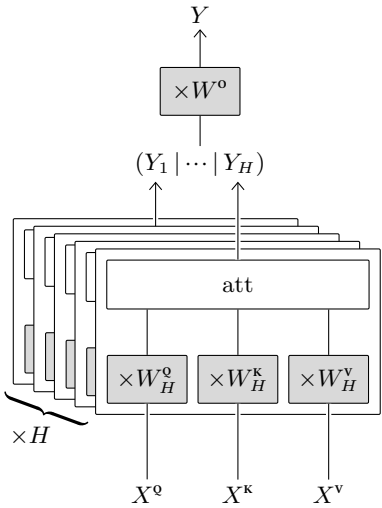

Figure 4.12: *The Multi-head Attention Layer applies for each of its $h = 1, \ldots, H$ heads a parametrized linear transformation to individual elements of the input sequences $X^{\mathrm{q}}, X^{\mathrm{k}}, X^{\mathrm{v}}$ to get sequences Q, K, V that are processed by the attention operator to compute Y_h. These H sequences are concatenated along features, and individual elements are passed through one last linear operator to get the final result sequence Y.*

- W^{Q} of size $H \times D \times D^{\mathrm{QK}}$,
- W^{K} of size $H \times D \times D^{\mathrm{QK}}$,
- W^{V} of size $H \times D \times D^{\mathrm{V}}$,

to compute respectively the queries, the keys, and the values from the input, and a final weight matrix W^{O} of size $HD^{\mathrm{V}} \times D$ to aggregate the per-head results.

It takes as input three sequences

- X^{Q} of size $N^{\mathrm{Q}} \times D$,
- X^{K} of size $N^{\mathrm{KV}} \times D$, and
- X^{V} of size $N^{\mathrm{KV}} \times D$,

from which it computes, for $h = 1, \ldots, H$

$$Y_h = \mathrm{att}\left(X^{\mathrm{Q}} W_h^{\mathrm{Q}}, X^{\mathrm{K}} W_h^{\mathrm{K}}, X^{\mathrm{V}} W_h^{\mathrm{V}}\right). \tag{4.12}$$

These sequences $Y_1, \ldots, Y_H$ are concatenated along the feature dimension and each individual element of the resulting sequence is multiplied by W^{O} to get the final result

$$Y = (Y_1 \mid \cdots \mid Y_H) W^{\mathrm{O}}. \tag{4.13}$$

It is noteworthy that the attention operator, and consequently the multi-head attention layer, is

invariant to a permutation of the keys and values, and equivariant to a permutation of the queries, as it would permute the resulting tensor similarly.

4.9 Token embedding

In many situations, we need to convert discrete tokens into vectors. This can be done with an embedding layer which consists of a lookup table that directly maps integers to vectors.

Such a layer is defined by two meta-parameters: the number N of possible token values, and the dimension D of the output vectors, and one trainable $N \times D$ weight matrix M.

Given as input an integer tensor X of dimension $D_1 \times \cdots \times D_K$ and values in $\{0,\ldots,N-1\}$ such a layer returns a real-valued tensor Y of dimension $D_1 \times \cdots \times D_K \times D$ with

$$\forall d_1,\ldots,d_K, \quad Y[d_1,\ldots,d_K] = M[X[d_1,\ldots,d_K]]. \quad (4.14)$$

4.10 Positional encoding

While the processing of a fully connected layer is specific to both the positions of the features in the input tensor, and to the position of the resulting activation in the output tensor, convolutional layers and multi-head attention layers are oblivious to the absolute position in the tensor. This is key to their strong invariance and inductive bias, which is beneficial to deal with a stationary signal.

However this can be an issue in certain situations where a proper processing has to access the absolute positioning. This is the case for instance for image synthesis, where the statistics of a scene is not totally stationary, or in natural language processing where the relative positions of words strongly modulate the meaning of a sentence.

The standard way to cope with this problem is to add or concatenate to the feature representation, at every position, a positional encoding, that is a feature vector that depends on the location, and allows to recover it. It can be learned as other layer parameters, or defined analytically.

For instance for a series of vectors of dimension

D, Vaswani et al. [2017] add

$$\text{pos-enc}[t,d] = \begin{cases} \sin\left(\frac{t}{T^{d/D}}\right) & \text{if } d \in 2\mathbb{N} \\ \cos\left(\frac{t}{T^{(d-1)/D}}\right) & \text{otherwise,} \end{cases} \tag{4.15}$$

with $T = 10^4$.

Chapter 5

Architectures

The field of deep learning has developed through the years for each application domain multiple deep architectures that exhibit good trade-off with respect to multiple criteria of interest: e.g. ease of training, accuracy of prediction, memory footprint, computational cost, scalability.

5.1 Multi-Layer Perceptrons

The simplest deep architecture is the Multi-Layer Perceptron (MLP), which takes the form of a succession of fully connected layers separated by activation functions. See an example on Figure 5.1. For historical reasons, in such a model, the number of hidden layers refers to the number of linear layers, excluding the last one.

A key theoretical result is the universal approximation theorem [Cybenko, 1989] that states that if the activation function σ is not polynomial, any continuous function f can be approximated

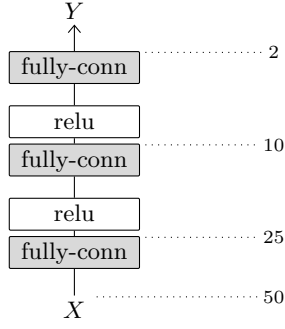

Figure 5.1: *This multi-layer perceptron takes as input a one dimension tensor of size* 50*, is composed of three fully connected layers with outputs of dimensions respectively* 25*,* 10*, and* 2*, the two first followed by ReLU layers.*

arbitrarily well uniformly on a compact by a model of the form $l_2 \circ \sigma \circ l_1$ where l_1 and l_2 are affine. Such a model is a MLP with a single hidden layer, and this result implies that it can approximate anything of practical value. However this approximation holds if the dimension of the first linear layer's output can be arbitrarily large.

In spite of their simplicity, MLPs remain an important tool when the dimension of the signal to process is not too large.

5.2 Convolutional networks

The standard architecture for processing images is a convolutional network, or convnet, that combines multiple convolutional layers, either to reduce the signal size before it can be processed by fully connected layers, or to output a 2d signal also of large size.

LeNet-like

The original LeNet model for image classification [LeCun et al., 1998] combines a series of 2d convolutional layers and max pooling layers that play the role of feature extractor, with a series of fully connected layers which act like a MLP and performs the classification per se. See Figure 5.2 for an example.

This architecture was the blueprint for many models that share its structure and are simply larger, such as AlexNet [Krizhevsky et al., 2012] or the VGG family [Simonyan and Zisserman, 2014].

Residual networks

Standard convolutional neural networks that follow the architecture of the LeNet family are not easily extended to deep architectures and suffer from the vanishing gradient problem. The resid-

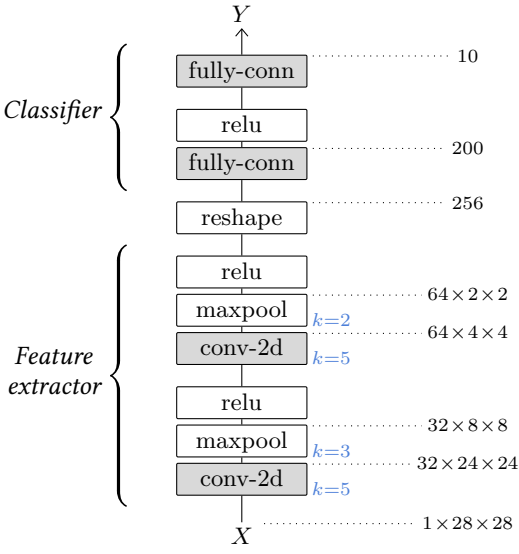

Figure 5.2: *Example of a small LeNet-like network for classifying* 28×28 *grayscale images of handwritten digits [LeCun et al., 1998]. Its first half is convolutional, and alternates convolutional layers per se and max pooling layers, reducing the signal dimension for* 28×28 *scalars to* 256*. Its second half processes this* 256 *dimension feature vector through a one hidden layer perceptron to compute* 10 *logit scores corresponding to the ten possible digits.*

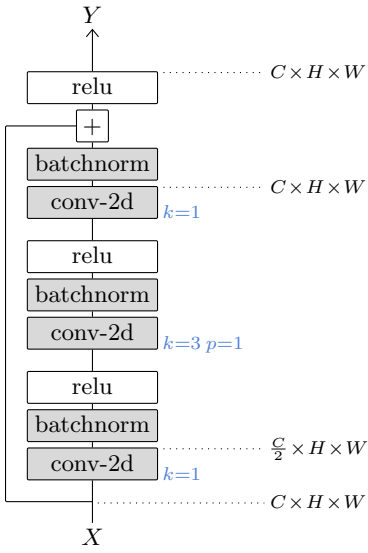

Figure 5.3: *A residual block.*

ual networks, or resnets, proposed by He et al. [2015] explicitly address the issue of the vanishing gradient with residual connections (see § 4.7), that allow hundreds of layers. They have become standard architectures for computer vision applications, and exist in multiple versions depending on the number of layers. We are going to look in detail at the architecture of the ResNet-50 for classification.

As other resnets, it is composed of a series of

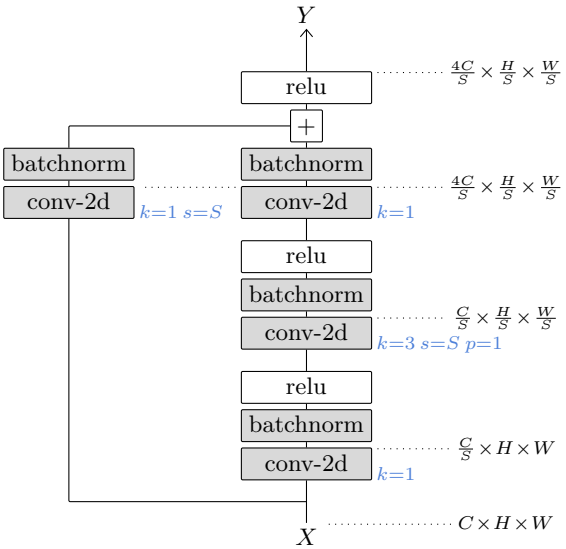

Figure 5.4: *A downscaling residual block. It admits a meta-parameter S, the stride of the first convolution layer, which modulates the reduction of the tensor size.*

residual blocks, each of them combining several convolutional layers, batch norm layers, and ReLU layers, wrapped into a residual connection. Such a block is pictured on Figure 5.3.

A key requirement for high performance with real images is to propagate a signal with a large number of channels, to allow a rich representation. However the parameter count of a con-

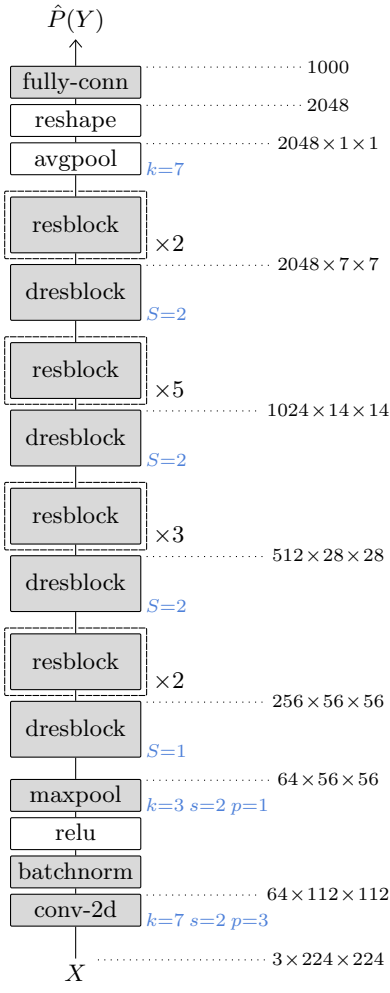

Figure 5.5: *Structure of the ResNet-50 [He et al., 2015].*

volutional layer, and its computational cost, are quadratic with the number of channels. This residual block mitigates this problem by first reducing the number of channels with a 1×1 convolution, then operating spatially with a 3×3 convolution on this reduced number of channels, and then up-scaling the number of channels, again with a 1×1 convolution.

The network reduces the dimensionality of the signal to finally compute the logits for the classification. This is done thanks to an architecture composed of several sections, each starting with a downscaling residual block that halves the height and width of the signal, and doubles the number of channels, followed by a series of residual blocks. Such a downscaling residual block has a structure similar to a standard residual block, except that it requires a residual connection that changes the tensor shape. This is achieved with a 1×1 convolution with a stride of two, see Figure 5.4.

The overall structure of the ResNet-50 is presented on Figure 5.5. It starts with a 7×7 convolutional layer that converts the three channel input image to a 64 channel image of half the size, followed by four sections of residual blocks. Surprisingly, in the first section, there

is no downscaling, only an increase of the number of channels by a factor of 4. The output of the last residual block is $2048 \times 7 \times 7$, which is converted to a vector of dimension 2048 by an average pooling of kernel size 7×7, and then processed through a fully connected layer to get the final logits, here for 1000 classes.

5.3 Attention models

As stated in § 4.8, many applications, in particular from natural language processing, greatly benefit from models that include attention mechanisms. The architecture of choice for such tasks, which has been instrumental in recent advances in deep learning, is the Transformer proposed by Vaswani et al. [2017].

Transformer

The original Transformer, pictured on Figure 5.7, was designed for sequence-to-sequence translation. It combines an encoder that processes the input sequence to get a refined representation, and an auto-regressive decoder that generates each token of the result sequence, given the encoder's representation of the input sequence, and the output tokens generated so far. As the residual convolutional networks of § 5.2, both the encoder and the decoder of the Transformer are sequences of compounded blocks built with residual connections.

The self-attention block, pictured on the left of Figure 5.6, combines a multi-head attention layer that recombine information globally, allowing any position to collect information from any other positions, with a one hidden layer MLP

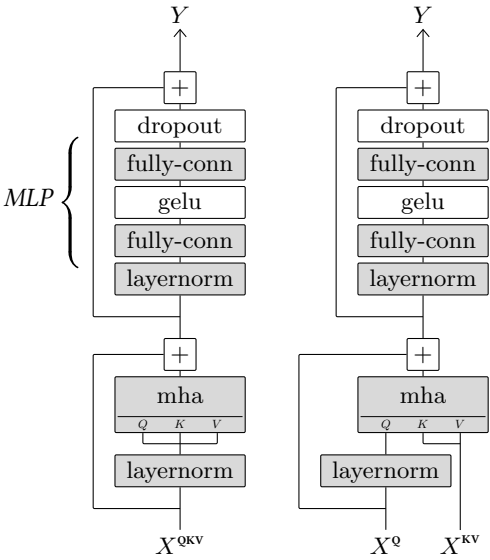

Figure 5.6: *Self-attention block (left) and cross-attention block (right). This specific structures proposed by Radford et al. [2018] differ slightly from the original architecture of Vaswani et al. [2017], in particular by having the* layernorm *as the first layer of the residual blocks.*

that updates representations at every position separately.

The cross-attention block, pictured on the right of Figure 5.6, is similar except that it takes as input two sequences, one to compute the queries,

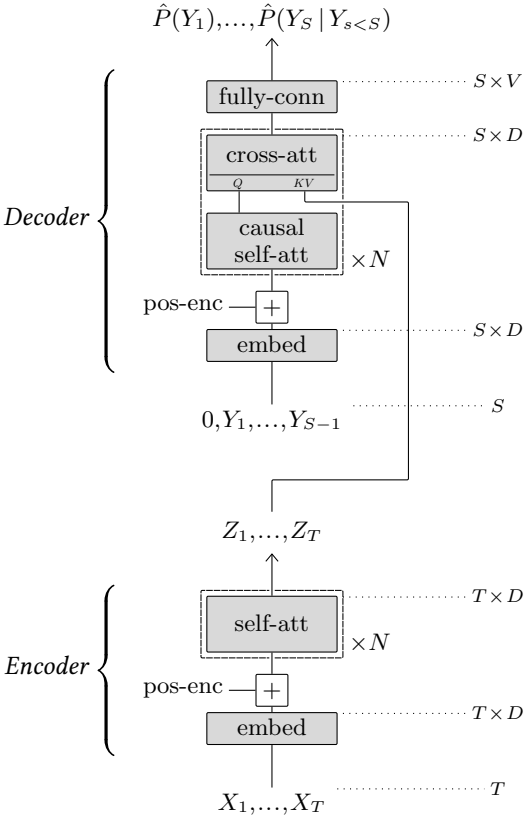

Figure 5.7: *Original encoder-decoder Transformer model for sequence-to-sequence translation [Vaswani et al., 2017].*

and one the keys and values.

The encoder of the Transformer processes the input sequence of discrete tokens $X_1, \ldots X_T$ through several self-attention blocks to generate a representation $Z_1, \ldots, Z_T$, and its decoder takes as input the sequence $Y_1, \ldots, Y_{S-1}$ of result tokens produced so far, and processes it through alternating causal self-attention blocks, and cross-attention blocks, to produce the logits predicting the next tokens. These cross-attention blocks compute their keys and values from the encoder's result representation of the input sequence, which allows the resulting sequence to be a function of it.

Thanks to the causal structure of the decoder, training the model consists of optimizing it such that, for any training input sequence X, the cross entropy loss summed over all the output tokens is minimized. This allows the autoregressive generation of the result sequence, see § 3.2.

Generative Pre-trained Transformer

The Generative Pre-trained Transformer (GPT, Radford et al., 2018, 2019), pictured on Figure 5.8 is a pure autoregressive model that consists of a succession of causal self-attention blocks, hence a causal version of the original Transformer en-

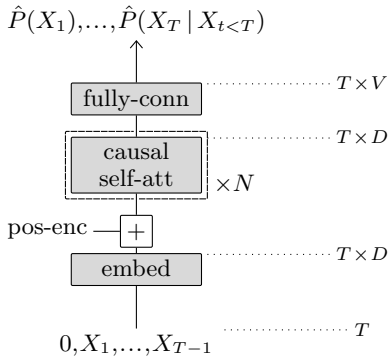

Figure 5.8: *GPT model [Radford et al., 2018].*

coder. This class of models scales extremely well, up to hundreds of billions of trainable parameters [Brown et al., 2020].

Vision Transformer

Transformers have been put to use for image classification with the Vision Transformer (ViT) model [Dosovitskiy et al., 2020], see Figure 5.9.

It splits the three-channel input image into M patches of resolution $P \times P$, that it flattens to create a sequence of vectors $X_1, \ldots, X_M$ of shape $M \times 3P^2$. This sequence is multiplied by a trainable matrix W^{E} of shape $3P^2 \times D$ to map it to a $M \times D$ sequence, to which is concatenated one trainable vector E_0. The resulting $(M+1) \times D$

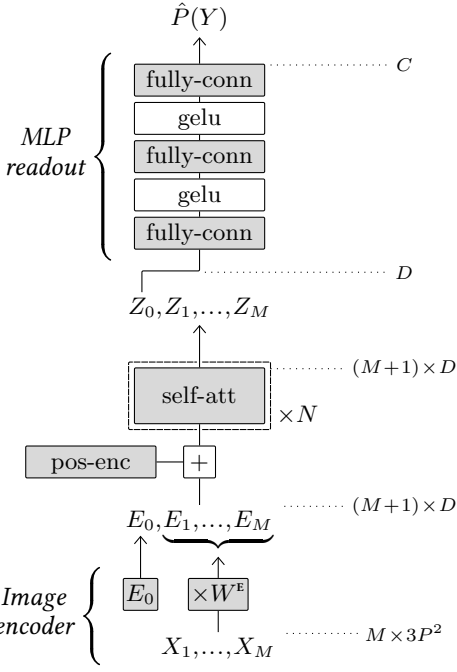

Figure 5.9: *Vision Transformer model [Dosovitskiy et al., 2020].*

sequence $E_0, \ldots, E_M$ is then processed through multiple self-attention blocks. See § 5.3 and Figure 5.6.

The first element Z_0 in the result sequence, which corresponds to E_0 and is not associated to any part of the image, is finally processed by a two hidden layer MLP to get the final C logits. Such a token added for a readout of a class prediction was introduced by Devlin et al. [2018] in the BERT model and is referred to as a CLS token.

Part III

Applications

Chapter 6

Prediction

A first category of applications such as face recognition, sentiment analysis, object detection, or speech recognition, requires to predict an unknown value from an available signal.

6.1 Image denoising

A direct application of deep models to image processing is to recover from degradation by using the redundancy in the statistical structure of images. The petals of a sunflower on a grayscale picture can be colored with high confidence, and the texture of a geometric shape such as a table on a low-light grainy picture can be corrected by averaging it over a large area likely to be uniform.

A denoising autoencoder is a model that takes as input a degraded signal $\tilde{X}$ and computes an estimate of the original one X.

Such a model is trained by collecting a large number of clean samples paired with their degraded inputs. The latters can be captured in degraded conditions, such as low-light or inadequate focus, or generated algorithmically, for instance by converting the clean sample to grayscale, reducing its size, or compressing it aggressively with a lossy compression method.

The standard training procedure for denoising autoencoders uses the MSE loss, in which case the model aims at computing $\mathbb{E}(X \mid \tilde{X})$. This quantity may be problematic when X is not totally determined by $\tilde{X}$, in which case some parts

of the generated signal may be an unrealistic blurry average.

6.2 Image classification

Image classification is the simplest strategy to extract semantic from an image and consists of predicting a class among a finite, predefined number of classes, given an input image.

The standard models for this task are convolutional networks, such as ResNets, see § 5.2, and attention-based models such as ViT, see § 5.3. Those models generate a vector of logits with as many dimensions as there are classes.

The training procedure simply minimizes the cross-entropy loss, see § 3.1. Usually performance can be improved with data augmentation, which consists of modifying the training samples with hand-designed random transformations, that do not change the semantic content of the image, such as cropping, scaling, mirroring, or color changes.

6.3 Object detection

A more complex task for image understanding is object detection, in which case the objective is, given an input image, to predict the classes and positions of objects of interest.

An object position is formalized as the four coordinates (x_1, y_1, x_2, y_2) of a rectangular bounding box, and the ground truth associated to each training image is a list of such bounding boxes, each labeled with the class of the object in it.

The standard approach to solve this task, for instance by the Single Shot Detector (SSD, Liu et al., 2015), is to use a convolutional neural network that produces a sequence of image representations Z_s of size $D_s \times H_s \times W_s$, $s = 1, \dots, S$, with decreasing spatial resolution $H_s \times W_s$ down to 1×1 for $s = S$, see Figure 6.1. Each of those tensors covers the input image in full, so the h, w indices correspond to a partitioning of the image lattice into regular squares that gets coarser when s increases. As seen in § 4.2, and illustrated on Figure 4.4, due to the succession of convolutional layers, a feature vector $(Z_s[0, h, w], \dots, Z_s[D_s - 1, h, w])$ is a descriptor of an area of the image, called its receptive field, that is larger than this square but centered on it. This results in a non-ambiguous matching of

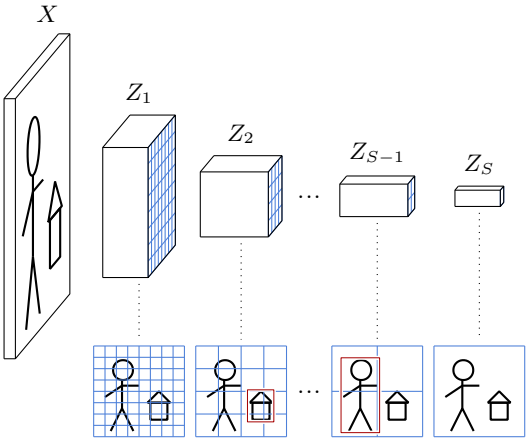

Figure 6.1: *A convolutional object detector processes the input image to generate a sequence of representations of decreasing resolutions. It computes for every h, w, at every scale s, a pre-defined number of bounding boxes whose centers are in the image area corresponding to that cell, and whose size is such that they fit in its receptive field. Each prediction takes the form of the estimates $(\hat{x}_1, \hat{x}_2, \hat{y}_1, \hat{y}_2)$, represented by the red boxes above, and a vector of $C+1$ logits for the C classes of interest, and an additional "no object" class.*

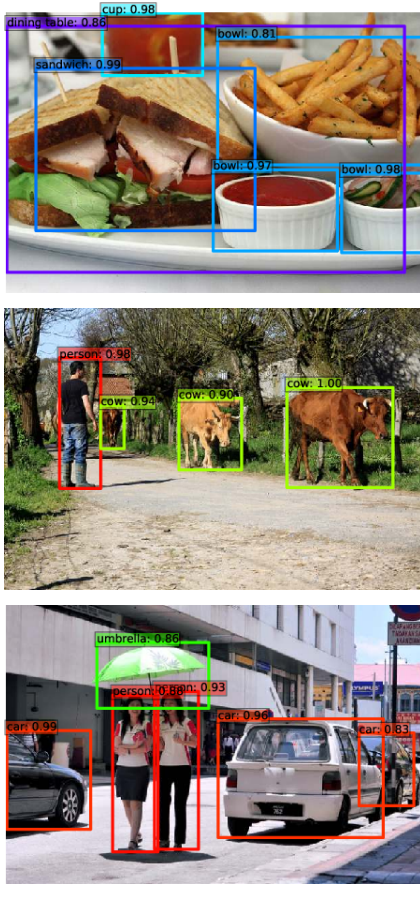

Figure 6.2: *Examples of object detection with the Single-Shot Detector [Liu et al., 2015].*

any bounding box (x_1, x_2, y_1, y_2) to a s, h, w, determined respectively by $\max(x_2 - x_1, y_2 - y_1)$, $\frac{y_1+y_2}{2}$, and $\frac{x_1+x_2}{2}$.

Detection is achieved by adding S convolutional layers, each processing a Z_s and computing for every tensor indices h, w the coordinates of a bounding box, and the associated logits. If there are C object classes, there are $C+1$ logits, the supplementary one standing for "no object." Hence each additional convolution layers has $4+C+1$ output channels. The SSD algorithm in particular generates several bounding boxes per s, h, w, each dedicated to a hard-coded range of aspect-ratios.

Training sets for object detection are costly to create, since the labeling with bounding boxes requires a slow human intervention. To mitigate this issue, the standard approach is to start with a convolutional model that has been pre-trained on a large classification data set such as VGG-16 for the original SSD, and to replace its final fully connected layers by additional convolutional ones. Surprisingly, models trained for classification only have learned feature representations that can be re-purposed for object detection, even though that task involves the regression of geometric quantities.

During training every ground truth bounding box is associated to its s, h, w, and induces a loss term composed of a cross entropy loss for the logits, and a regression loss such as MSE for the bounding box coordinates. Every other s, h, w free of bounding-box match induces a cross-entropy only penalty to predict the class "no object".

6.4 Semantic segmentation

The finest grain prediction task for image understanding is semantic segmentation, which consists of predicting for every pixel the class of the object it belongs to. This can be achieved with a standard convolutional neural network, that outputs a convolutional map with as many channels as classes, that carry the estimated logits for every pixel.

While a standard residual network for instance can generate a dense output of same resolution as its input, as for object detection, this task requires to operate at multiple scales. This is necessary so that any object, or sufficiently informative sub-part, whatever its size, is captured somewhere in the model by the feature representation at a single tensor position. Hence, standard architectures for that task downscale the image with a series of convolutional layers, to increase the receptive field of the activations, and re-upscale it with a series of transposed convolutional layers, or other upscaling methods such as bilinear interpolation to make the prediction at high resolution.

However, a strict downscaling-upscaling architecture does not allow to operate at a fine grain when making the final prediction, since all the

Figure 6.3: *Semantic segmentation results with the Pyramid Scene Parsing Network [Zhao et al., 2016].*

signal has been transmitted through a low resolution representation at some point. Models that apply such downscaling-upscaling serially have skip connections from layers at a certain resolution, before downscaling, to layers at the same resolution, after upscaling [Long et al., 2014; Ronneberger et al., 2015]. Models that do it in parallel, after a convolutional backbone, concatenate the resulting multi-scale representation after up-

scaling, before making the final per-pixel prediction [Zhao et al., 2016].

Training is achieved with a standard cross-entropy summed over all the pixels. As for object detection, training can start from a network pre-trained on a large-scale image classification data set to compensate for the limited availability of segmentation ground-truth.

6.5 Speech recognition

Speech recognition consists of converting a sound sample into a sequence of words. There have been plenty of approaches to this problem historically, but a conceptually simple and recent one consists of casting it as a sequence-to-sequence translation and then solving it with a standard attention-based Transformer.

The model proposed by Radford et al. [2022] first converts the sound signal into a spectrogram, which is a one dimension series $T \times D$, that encodes at every time step a vector of energies in D frequency bands.

This sequence is processed through a few 1d convolutional layers, and the resulting representation is fed into the encoder of the Transformer. The decoder directly generates a discrete sequence of tokens, that correspond to one of the possible tasks considered during training. Multiple objectives are considered for training: transcription of English or non-English text, translation from any language to English, or a detection of non-speech sequences, such as background music or ambient noise.

This approach allows to leverage extremely large data sets that combine multiple types of sound

sources with diverse ground truth.

6.6 Text-image representations

A powerful approach to image understanding consists of learning consistent image and text representations.

The Contrastive Language Image Pre-training (CLIP) proposed by Radford et al. [2021] combines an image encoder f, which can be a ResNet-50, see § 5.2, and a text encoder g, which is a GPT, see § 5.3. To use a GPT as a text encoder, instead of a standard autoregressive model, they add to the input sequence an "end of sentence" token, and use the representation of this token in the last layer as the embedding. Both embeddings have the same dimension which, depending on the configuration, is between 512 and 1024.

Those two models are trained from scratch from a data set of 400 million image-text pairs (i_k, t_k) collected from the internet. The training procedure follows the standard mini batch stochastic gradient descent approach but relies on a contrastive loss. The embeddings are computed for every image and every text of the N pairs in the mini-batch, and a cosine similarity measure is computed not only between text and image embeddings from each pair, but also across pairs,

resulting in a $N \times N$ matrix of similarity score

$$l_{m,n} = f(i_m)^\top g(t_n),\ m = 1,\ldots,N, n = 1,\ldots,N.$$

The model is trained with cross entropy so that, for $\forall n$ the values $l_{1,n},\ldots,l_{N,n}$ interpreted as logit scores predict n, and similarly for $l_{n,1},\ldots,l_{n,N}$.

This means in practice that $\forall n, m,$ s.t. $n \neq m$ the similarity $l_{n,n}$ is unambiguously greater than both $l_{n,m}$ and $l_{m,n}$.

When it has been trained, this model can be used to do zero-shot prediction, that is classifying a signal in absence of training examples by defining a series of candidate classes with text descriptions, and computing the similarity of the embedding of an image with the embedding of each of those descriptions. See Figure 6.4.

Additionally, since the textual descriptions are often detailed, such a model has to capture richer representation of images, and pick up cues overlooked by classifier networks. This translates to excellent performance on challenging datasets such as ImageNet Adversarial [Hendrycks et al., 2019] which was specifically designed to degrade or erase cues on which standard predictors rely.

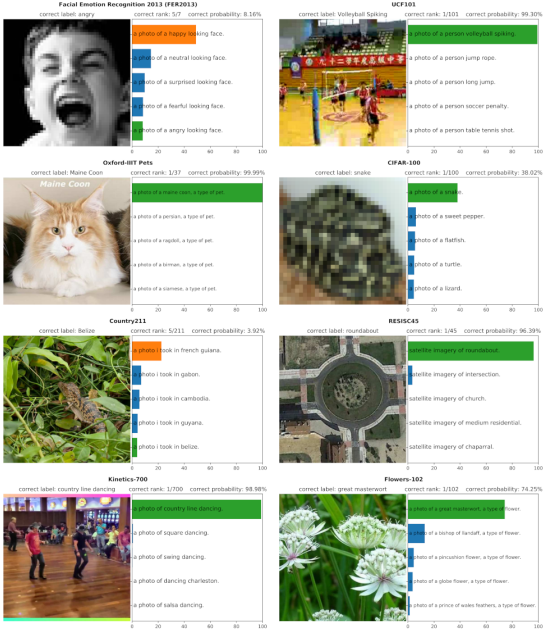

Figure 6.4: *The CLIP text-image embedding [Radford et al., 2021] allows to do zero-shot prediction by predicting what class description embedding is the most consistent with the image embedding.*

Chapter 7

Synthesis

A second category of applications distinct from prediction is synthesis. It consists of fitting a density model to training samples, and providing means to sample from this model.

7.1 Text generation

The standard approach to text synthesis is to use an attention-based autoregressive model. The most successful in this domain is the GPT [Radford et al., 2018], that we described in § 5.3.

As we saw in § 3.2, such a model takes as input a series of discrete tokens, and computes a series of as many vectors of logits, each with as many dimensions as the vocabulary size. By design this model is causal, which means that the quantities it computes at a certain position t in the output sequence depend only on the tokens that appear before t in the input sequence. This ensures that, given a full input sequence, the output at every position is the prediction that would have been obtained if the input was only available until just before that position.

When it has been trained on very large datasets, such a simple language model exhibits extremely powerful properties. Besides the syntactic and grammatical structure of the language, it has to integrate very diverse knowledge, e.g. to predict the word following "The capital of Japan is", "if water is heated to 100 Celsius degrees it turns into", or "because her puppy was sick, Jane was".

More surprising, when such a model is put

in a statistical context by a "prompt" carefully crafted, it can exhibit abilities for question answering, problem solving, and chain-of-thought that appear eerily close to high-level reasoning [Chowdhery et al., 2022; Bubeck et al., 2023].

7.2 Image generation

Multiple deep methods have been developed to model and sample from a high dimension density. A powerful one for image synthesis relies on inverting a diffusion process.

The principle consists of defining analytically a process that gradually degrades any sample, and consequently transforms the complex and unknown density of the data, into a simple and well-known density such as a normal, and to train a deep architecture to invert this degradation process [Ho et al., 2020].

In practice, given a fixed T, the diffusion process defines a probabilities over series of $T+1$ samples as follows: samples x_0 uniformly in the data set, and then go on sampling $x_{t+1} \sim p(x_{t+1} \mid x_t)$ where p is analytically defined and such that it gradually erases the structure that was in x_0. The setup should be such that the distribution $p(x_T)$ of x_T is known, so in particular does not depend on $p(x_0)$, and can be sampled.

For instance, in the setup of Ho et al. [2020], the data is normalized to mean 0 and variance 1, and the diffusion process consists of adding a bit of white noise and re-normalizing the variance to 1. This process reduces exponentially the im-

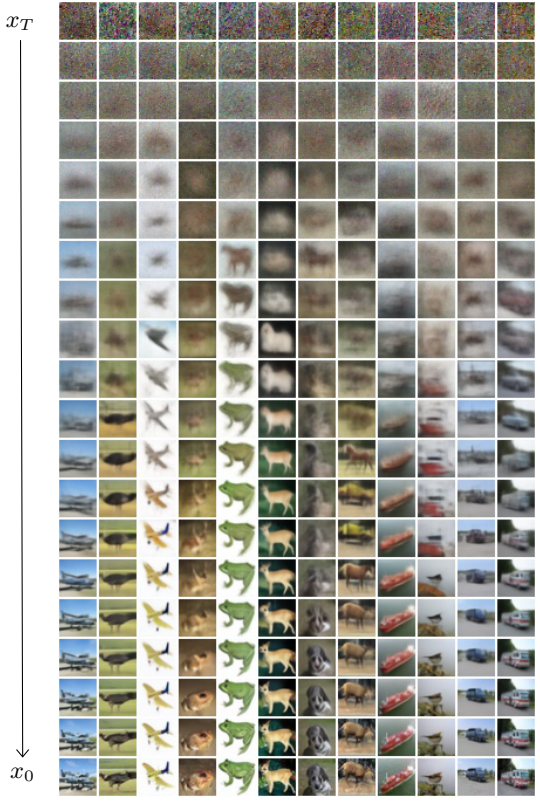

Figure 7.1: *Image synthesis with denoising diffusion [Ho et al., 2020]. Each sample starts as a white noise x_T (top), and is gradually de-noised by sampling iteratively $x_{t-1} \mid x_t \sim \mathcal{N}(x_t + f(x_t, t; w), \sigma_t)$.*

portance of x_0, and x_t's density can rapidly be approximated with a normal.

The denoiser f is a deep architecture that should model, and allow to sample from, $f(x_{t-1}, x_t, t; w) \simeq p(x_{t-1} \mid x_t)$. It can be shown that if this one step reverse process is accurate enough, sampling $x_T \sim p(x_T)$ and denoising T steps with f results in a x_0 that follows $p(x_0)$.

Training f can be achieved by generating a large number of sequences $x_0^{(n)}, \ldots, x_T^{(n)}$, picking a t_n in each, and maximizing

$$\sum_n \log f(x_{t_n-1}^{(n)}, x_{t_n}^{(n)}, t_n; w).$$

Given the form of their diffusion process, Ho et al. [2020] have a denoising of the form

$$x_{t-1} \mid x_t \sim \mathcal{N}(x_t + f(x_t, t; w); \sigma_t),$$

where σ_t is defined analytically.

In practice, what such a model does is to initially hallucinate structures by pure luck in the random noise, and then gradually builds more elements that emerge from the noise by reinforcing the most likely continuation of the image obtained so far.

The missing bits

For the sake of concision, this volume skips a lot of important topics, in particular:

• Recurrent Neural Networks (RNN) were the standard approach to deal with temporal sequences such as text or sound samples, before attention models demonstrated greater performance. These architectures possess an internal hidden state, that get updated every time a component of the sequence get processed. Their main components are layers such as LSTM [Hochreiter and Schmidhuber, 1997] or GRU [Cho et al., 2014]. Training a recurrent architecture amounts to unfolding it in time, which results in a long composition of operators. This historically prompted the design of key techniques now used for deep architectures such as rectifiers and gating, a form of skip connections

which are modulated dynamically.

• An autoencoder is a model that maps the input signal, possibly of high dimension, to a low-dimension latent representation, and maps it back to the original signal, ensuring that information has been preserved. We saw it in § 6.1 for denoising, but it can be used to discover automatically a meaningful low-dimension parameterization of the data manifold. The Variational Autoencoder (VAE) proposed by Kingma and Welling [2013] has a similar structure, but imposes through the loss a distribution to the latent representation. After training, it allows to generate signals by sampling the latent representation according to this imposed distribution, and then mapping back through the decoder.

• Generative Adversarial Networks (GAN) introduced by Goodfellow et al. [2014] are another approach to density modeling. It combines a generator, that takes a random input following a fixed distribution as input and produces a structured signal such as an image, and a discriminator, that takes as input a sample and predicts if it comes from the training set, or if it was generated by the generator. Training optimizes the discriminator to minimize a standard cross-entropy loss, and the generator to maximize the

discriminator's loss. It can be shown that at the equilibrium the generator produces samples indistinguishable from real data. In practice, when the gradient flows through the discriminator to the generator, it informs the latter about the cues that the discriminator uses, that should be fixed.

• Reinforcement Learning (RL) trains a model to estimate an accumulated long-term reward given action choices and an observable state, and what actions to choose to maximize that reward. Many problems, for instance strategy games or robotic control, can be formulated in that framework. Deep models, in particular convolutional neural networks, have demonstrated excellent performance for this class of tasks [Mnih et al., 2015].

• Fine-tuning deep architectures is an efficient strategy to deal with small training sets for certain tasks, such as object detection or semantic segmentation, as we saw in § 6.3 and § 6.4. Beside, due to the dramatic increase in the size of architectures, particularly attention models, training a single model can cost several millions of dollars, and fine-tuning is a crucial, and often the only way, to achieve high performance on a specific task.

Afterword

Recent developments in Artificial Intelligence have been incredibly exciting, and it is difficult to comment on them without being overly dramatic. There are few doubts that these technologies will trigger fundamental changes in how we work, how we interact with knowledge and information, and that they will force us to rethink concepts as fundamental as intelligence, understanding, and sentience.

In spite of its weaknesses, in particular its sheer brutality and its computational cost, deep learning is likely to remain an important component of AI systems for the foreseeable future and, as such, a key element of this new era.

Bibliography

J. L. Ba, J. R. Kiros, and G. E. Hinton. Layer Normalization. *CoRR*, abs/1607.06450, 2016. [pdf]. 67

A. Baydin, B. Pearlmutter, A. Radul, and J. Siskind. Automatic differentiation in machine learning: a survey. *CoRR*, abs/1502.05767, 2015. [pdf]. 36

M. Belkin, D. Hsu, S. Ma, and S. Mandal. Reconciling modern machine learning and the bias-variance trade-off. *CoRR*, abs/1812.11118, 2018. [pdf]. 39

T. Brown, B. Mann, N. Ryder, et al. Language Models are Few-Shot Learners. *CoRR*, abs/2005.14165, 2020. [pdf]. 21, 95

S. Bubeck, V. Chandrasekaran, R. Eldan, et al. Sparks of Artificial General Intelligence:

Early experiments with GPT-4. *CoRR*, abs/2303.12712, 2023. [pdf]. 118

T. Chen, B. Xu, C. Zhang, and C. Guestrin. Training Deep Nets with Sublinear Memory Cost. *CoRR*, abs/1604.06174, 2016. [pdf]. 36

K. Cho, B. van Merrienboer, Ç. Gülçehre, et al. Learning Phrase Representations using RNN Encoder-Decoder for Statistical Machine Translation. *CoRR*, abs/1406.1078, 2014. [pdf]. 122

A. Chowdhery, S. Narang, J. Devlin, et al. PaLM: Scaling Language Modeling with Pathways. *CoRR*, abs/2204.02311, 2022. [pdf]. 21, 118

G. Cybenko. Approximation by superpositions of a sigmoidal function. *Mathematics of Control, Signals, and Systems*, 2(4):303–314, December 1989. [pdf]. 82

J. Devlin, M. Chang, K. Lee, and K. Toutanova. BERT: Pre-training of Deep Bidirectional Transformers for Language Understanding. *CoRR*, abs/1810.04805, 2018. [pdf]. 21, 97

A. Dosovitskiy, L. Beyer, A. Kolesnikov, et al. An Image is Worth 16x16 Words: Transformers for Image Recognition at Scale. *CoRR*, abs/2010.11929, 2020. [pdf]. 95, 96

K. Fukushima. Neocognitron: A self-organizing neural network model for a mechanism of pattern recognition unaffected by shift in position. *Biological Cybernetics*, 36(4):193–202, April 1980. [pdf]. 2

Y. Gal and Z. Ghahramani. Dropout as a Bayesian Approximation: Representing Model Uncertainty in Deep Learning. *CoRR*, abs/1506.02142, 2015. [pdf]. 63

X. Glorot and Y. Bengio. Understanding the difficulty of training deep feedforward neural networks. In *International Conference on Artificial Intelligence and Statistics (AISTATS)*, 2010. [pdf]. 37, 48

X. Glorot, A. Bordes, and Y. Bengio. Deep Sparse Rectifier Neural Networks. In *International Conference on Artificial Intelligence and Statistics (AISTATS)*, 2011. [pdf]. 56

I. J. Goodfellow, J. Pouget-Abadie, M. Mirza, et al. Generative Adversarial Networks. *CoRR*, abs/1406.2661, 2014. [pdf]. 123

K. He, X. Zhang, S. Ren, and J. Sun. Deep Residual Learning for Image Recognition. *CoRR*, abs/1512.03385, 2015. [pdf]. 21, 68, 69, 86, 88

D. Hendrycks and K. Gimpel. Gaussian Error Linear Units (GELUs). *CoRR*, abs/1606.08415, 2016. [pdf]. 58

D. Hendrycks, K. Zhao, S. Basart, et al. Natural Adversarial Examples. *CoRR*, abs/1907.07174, 2019. [pdf]. 114

J. Ho, A. Jain, and P. Abbeel. Denoising Diffusion Probabilistic Models. *CoRR*, abs/2006.11239, 2020. [pdf]. 119, 120, 121

S. Hochreiter and J. Schmidhuber. Long Short-Term Memory. *Neural Computation*, 9(8):1735–1780, 1997. [pdf]. 122

S. Ioffe and C. Szegedy. Batch Normalization: Accelerating Deep Network Training by Reducing Internal Covariate Shift. In *International Conference on Machine Learning (ICML)*, 2015. [pdf]. 64

D. Kingma and J. Ba. Adam: A Method for Stochastic Optimization. *CoRR*, abs/1412.6980, 2014. [pdf]. 33

D. P. Kingma and M. Welling. Auto-Encoding Variational Bayes. *CoRR*, abs/1312.6114, 2013. [pdf]. 123

A. Krizhevsky, I. Sutskever, and G. Hinton. ImageNet Classification with Deep Convolutional

Neural Networks. In *Neural Information Processing Systems (NIPS)*, 2012. [pdf]. 8, 84

Y. LeCun, B. Boser, J. S. Denker, et al. Backpropagation applied to handwritten zip code recognition. *Neural Computation*, 1(4):541–551, 1989. [pdf]. 8

Y. LeCun, L. Bottou, Y. Bengio, and P. Haffner. Gradient-based learning applied to document recognition. *Proceedings of the IEEE*, 86(11): 2278–2324, 1998. [pdf]. 84, 85

W. Liu, D. Anguelov, D. Erhan, et al. SSD: Single Shot MultiBox Detector. *CoRR*, abs/1512.02325, 2015. [pdf]. 103, 105

J. Long, E. Shelhamer, and T. Darrell. Fully Convolutional Networks for Semantic Segmentation. *CoRR*, abs/1411.4038, 2014. [pdf]. 68, 69, 109

A. L. Maas, A. Y. Hannun, and A. Y. Ng. Rectifier nonlinearities improve neural network acoustic models. In *proceedings of the ICML Workshop on Deep Learning for Audio, Speech and Language Processing*, 2013. [pdf]. 57

V. Mnih, K. Kavukcuoglu, D. Silver, et al. Human-level control through deep reinforcement

learning. *Nature*, 518(7540):529–533, February 2015. [pdf]. 124

A. Radford, J. Kim, C. Hallacy, et al. Learning Transferable Visual Models From Natural Language Supervision. *CoRR*, abs/2103.00020, 2021. [pdf]. 113, 115

A. Radford, J. Kim, T. Xu, et al. Robust Speech Recognition via Large-Scale Weak Supervision. *CoRR*, abs/2212.04356, 2022. [pdf]. 111

A. Radford, K. Narasimhan, T. Salimans, and I. Sutskever. Improving Language Understanding by Generative Pre-Training, 2018. [pdf]. 92, 94, 95, 117

A. Radford, J. Wu, R. Child, et al. Language Models are Unsupervised Multitask Learners, 2019. [pdf]. 94

O. Ronneberger, P. Fischer, and T. Brox. U-Net: Convolutional Networks for Biomedical Image Segmentation. In *Medical Image Computing and Computer-Assisted Intervention*, 2015. [pdf]. 68, 69, 109

J. Sevilla, L. Heim, A. Ho, et al. Compute Trends Across Three Eras of Machine Learning. *CoRR*, abs/2202.05924, 2022. [pdf]. 9, 21

K. Simonyan and A. Zisserman. Very Deep Convolutional Networks for Large-Scale Image Recognition. *CoRR*, abs/1409.1556, 2014. [pdf]. 84

N. Srivastava, G. Hinton, A. Krizhevsky, et al. Dropout: A Simple Way to Prevent Neural Networks from Overfitting. *Journal of Machine Learning Research (JMLR)*, 15:1929–1958, 2014. [pdf]. 62

A. Vaswani, N. Shazeer, N. Parmar, et al. Attention Is All You Need. *CoRR*, abs/1706.03762, 2017. [pdf]. 68, 71, 80, 91, 92, 93

M. D. Zeiler and R. Fergus. Visualizing and Understanding Convolutional Networks. In *European Conference on Computer Vision (ECCV)*, 2014. [pdf]. 54

H. Zhao, J. Shi, X. Qi, et al. Pyramid Scene Parsing Network. *CoRR*, abs/1612.01105, 2016. [pdf]. 109, 110

Index